Available online at www.sciencedirect.com

Journal of Organometallic Chemistry 691 (2006) 1954–1964

Journal of Organometallic Chemistry

www.elsevier.com/locate/jorganchem

Structural characterization of rare intramolecularly (1,4-Te···N) bonded diorganotellurides and their monomeric complexes with mercury(II) halides: Metal assisted C–H···X (Hg) interactions leading to supramolecular architecture

Ashok K.S. Chauhan [a,*], Anamika [a], Arun Kumar [a], Puspendra Singh [a], Ramesh C. Srivastava [a], Ray J. Butcher [b], Jens Beckmann [c], Andrew Duthie [d]

[a] *Department of Chemistry, University of Lucknow, Lucknow 226 007, India*
[b] *Department of Chemistry, Howard University, Washington, DC 20059, USA*
[c] *Institut für Chemie, Freie Universität Berlin, Fabeckstrasse 34-36, 14195 Berlin, Germany*
[d] *Centre for Chiral and Molecular Technologies, Deakin University, Geelong 3217, Australia*

Received 22 October 2005; received in revised form 15 December 2005; accepted 3 January 2006

Abstract

Monomeric tellurides 4-$RC_6H_4(SB)Te$ [SB = 2-(4,4′-$NO_2C_6H_4CH{=}NC_6H_3$–Me); R = H, **1a**; Me, **1b**; OMe, **1c**], which incidentally represent the first example of a telluride with 1,4-Te···N intramolecular interaction, have been prepared and characterized by solution and solid-state ^{125}Te NMR, ^{13}C NMR and X-ray crystallography. Interplay of weak C–H···O and C–H···π interactions in the crystal lattice of **1b** and **1c** are responsible for the formation of supramolecular motifs. These tellurides undergo expected oxidative addition reactions with halogens and interhalogens and also interact coordinatively with mercury(II) halides to give 1:2 complexes, $HgX_2[4\text{-}RC_6H_4(SB)Te]_2$ (X = Cl, R = H, **2a**; Me, **2b**; OMe, **2c** and X = Br, R = H, **3a**; Me, **3b**; and OMe, **3c**) with no sign of Te–C bond cleavage, as has been reported for some 1,5-Te···N(O) intramolecularly bonded tellurides. The complexes **2a** and **3c** are the first structurally characterized monomeric 1:2 adducts of mercury(II) halides with Te ligands. The 1,4-Te···N intramolecular interactions in the solid-state are retained in the complexes highlighting simultaneously the Lewis acid and base character of the Te(II) atom. Packing of molecules in the crystal lattice of **2a** and **3c** reveals that non-covalent C–H···Cl/Br interactions involving metal-bound halogen atoms possess significant directionality and in combination with coordinative covalent interactions may be of potential use in creating inorganic supramolecular synthons.

Keywords: Intramolecular bonding; Non-covalent interactions; Mercury halide complex; Tellurium ligands; Crystal engineering; C–H···X interaction

---

1. Introduction

The role of intermolecular secondary bonding interactions (SBIs) as associative forces and that of intramolecular SBIs in the stability and reactivity of organotellurium compounds has been a subject of continuous investigations since the time of Alcock's observations and reviewed periodically [1–3]. The latter interactions also appear to influence the mode of reaction of the tellurides (R_2Te) with d^8 and d^{10} metal acceptors. At least four different products have been isolated in the reactions with mercury(II) halides as per the following equation:

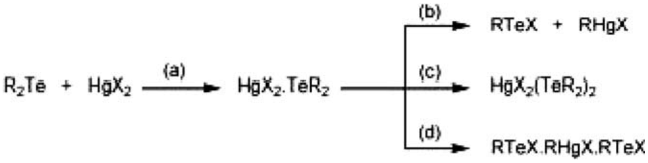

(1)

---

[*] Corresponding author.
E-mail address: akschauhan2003@yahoo.co.in (A.K.S. Chauhan).

doi:10.1016/j.jorganchem.2006.01.034

Formation of the transmetallation (reaction 1b) [4] and inclusion products (reaction 1d) [5] involve cleavage of a Te–C bond and have been suggested to be the consequence of intramolecular 1,5-Te···N(O) interactions leading to weakening of the *trans* Te–C bond. The 1:1 adducts (reaction 1a) are oligomeric and have been structurally characterized in a few cases [6]. Comparatively, fewer cases of the formation of 1:2 monomeric complexes, $HgX_2(R_2Te)_2$ (reaction 1c), have been observed and surprisingly none appears to have been crystallographically characterized so far. In this communication the synthesis and structural characterization of functionalized diorganotellurides involving 1,4-type intramolecular Te(II)···N interactions and their 1:2 complexes with mercury(II) halides are discussed. Our interest in 1,4-type intramolecular SBIs stems from a recent observation [7] that 1,4-Te···O interactions are present in the Te(IV) compounds $(4\text{-}RC_6H_4COCH_2)_2TeX_2$, but do not exist in the corresponding tellurides $(4\text{-}RC_6H_4COCH_2)_2Te$, which are stabilized by intermolecular Te···Te interactions in the solid-state. On the other hand, 1,5-Te···N(O) intramolecular SBIs have been found to be present in both Te(IV) and Te(II) derivatives. We were therefore interested to know (i) if 1,4-Te(IV)···N intramolecular interactions observed in the unsymmetrical diorganotellurium dihalides $(4\text{-}MeOC_6H_4)[2\text{-}(4,4'\text{-}NO_2C_6H_4\text{-}CHNC_6H_3Me)]TeX_2$, $R(SB)TeX_2$ [8], are retained in the corresponding diorganotellurides, R(SB)Te and (ii) if such an interaction also leads to weakening of Te–C bond *trans* to the nucleophilic nitrogen atom in the telluride and (iii) if so, is path (b) or (d) (Eq. (1)) followed. If formed, solid-state structural characterization of the 1:2 adduct (path 1c) was also an incentive due to the lack of previous crystallographic studies. An added interest in this study was investigation of the solid-state molecular packing of compounds **1a**–**c**, which are organotellurium(II) derivatives of 4-nitro-4′-methylbenzylideneaniline (NMBA), an organic substrate known to possess second-order non-linear (NLO) properties [9].

2. Results and discussion

The asymmetrical tellurides **1a**–**c** were prepared by the bisulfite reduction of the corresponding dichlorides, $(4\text{-}RC_6H_4)(SB)TeCl_2$. All the three tellurides are sharp melting red crystalline solids which are soluble in ether, dichloromethane and chloroform. The IR spectra of **1a**–**c** show an absorption band at ~1586 cm^{-1} due to $\nu(C{=}N)$ while the ^1H NMR spectra consist of, in addition to CH_3/OCH_3 and/or aryl protons, a low field (~8.7 ppm) signal for the methine proton. In the ^{13}C NMR spectra the methine carbon atom appears at ~144 ppm (Table 1). The signal at ~123 ppm can be assigned to the tellurated C atom of the nitrogen ring which is, as expected, deshielded compared to the free Schiff base (111.1 ppm). ^{125}Te chemical shifts of the tellurides **1a**–**c** and their mercury(II) halide complexes are listed in Table 2 which also includes data on the three bis(4-substituted benzoylmethyl)tellurides (preparation and characterization of which have been reported earlier

Table 1
^{13}C NMR data of tellurides **1** and their HgX_2 complexes **2** and **3**

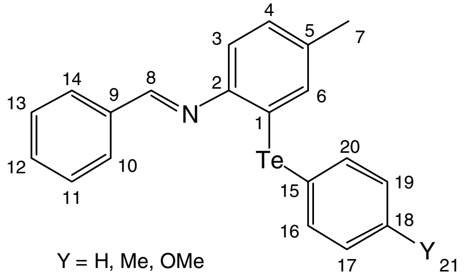

Entry no.	**1a**	**2a**	**3a**	**1b**	**2b**	**3b**	**1c**	**2c**	**3c**
C7	21.2	20.6	20.6	21.1	20.6	20.7	21.2	20.7	20.7
C21				21.5	21.0	21.0	55.2	54.9	54.8
C15	113.6	113.2	113.2	109.4	109.0	109.2	102.8	102.7	102.3
C3	115.7	116.1	116.1	115.5	116.1	116.6	115.8	116.3	116.0
C1	124.1	122.3	122.4	124.0	123.8	122.7	124.0	123.7	123.7
C10,11,13,14	128.8	128.3	128.3	128.2	128.1	128.3	128.2	128.8	128.3
C4	129.5	129.6	129.4	129.4	129.4	128.6	129.4	129.5	129.4
C9	129.9	132.3	132.2	131.0	131.9	131.9	132.9	132.2	132.0
		135.3	135.4		138.3	137.6			
C5	139.3	138.4	138.4	139.0	138.4	138.6	139.2	138.5	138.4
C6	141.4	141.1	141.1	141.5	140.9	141.3	141.4	141.1	141.1
C16,17,19,20	141.4	140.5	140.6	141.5	141.2	141.0	143.3	142.1	142.3
C2	146.5	146.1	146.1	146.5	146.0	146.2	146.3	146.1	145.9
C12	149.2	148.7	148.8	146.5	148.8	148.9	146.3	148.7	148.8
C8	154.3	155.8	155.9	154.2	155.9	156.5	154.8	156.3	155.8
C18	139.3	138.8	138.8	139.0	139.0	138.7	160.4	160.2	160.1

Table 2
Solution (d_6-DMSO) and solid-state ^{125}Te NMR chemical shifts for some tellurides and HgX$_2$ complexes **2** and **3**

Compound	δ (ppm)	δ_{iso} (ppm)
$(PhCOCH_2)_2Te$	484	
$(4\text{-}MeC_6H_4COCH_2)_2Te$	487	
$(4\text{-}MeOC_6H_4COCH_2)_2Te$	493	
Ph(SB)Te (**1a**)	593	573
$4\text{-}MeC_6H_4$(SB)Te (**1b**)	575	574
$4\text{-}MeOC_6H_4$(SB)Te (**1c**)	564	
[Ph(SB)Te]$_2$HgCl$_2$ (**2a**)	572	438, 467
[$4\text{-}MeC_6H_4$(SB)Te]$_2$HgCl$_2$ (**2b**)	559	
[$4\text{-}MeOC_6H_4$(SB)Te]$_2$HgCl$_2$ (**2c**)	533	417
[Ph(SB)Te]$_2$HgBr$_2$ (**3a**)	573	
[$4\text{-}MeC_6H_4$(SB)Te]$_2$HgBr$_2$ (**3b**)	556	
[$4\text{-}MeOC_6H_4$(SB)Te]$_2$HgBr$_2$ (**3c**)	538	

[7b]). ^{125}Te NMR spectra of all the tellurides (Table 2) consist of a single resonance indicating that the asymmetric molecules **1a**–**c** do not undergo disproportionation to the corresponding symmetric species in solution. In accordance with the increased electron density around Te in the tellurides, the ^{125}Te NMR chemical shifts for the tellurides are shifted to lower frequency in comparison to the Te(IV) dihalides [8] and also appear to follow the expected trend of alkyl tellurides, [$(4\text{-}RC_6H_4COCH_2)_2Te$] being lower than the aryl tellurides **1a**–**c**. The ^{125}Te CP MAS NMR spectra of Ph(SB)Te (**1a**) and $4\text{-}MeC_6H_4$(SB)Te (**1b**) revealed isotropic chemical shifts at 573 and 574 ppm, respectively, which are close to those observed for their DMSO solutions.

The tellurides (**1a**–**c**) are readily oxidized by SO_2Cl_2, Br_2 and I_2 at 0 °C to the corresponding Te(IV) dihalides, [$4\text{-}RC_6H_4$(SB)TeX$_2$], which had earlier been prepared by a transmetallation reactions between (SB)HgCl and ($4\text{-}RC_6H_4$)TeCl$_3$ (in the case of X = Cl) or by the halide exchange between ($4\text{-}RC_6H_4$)(SB)TeCl$_2$ and KBr or KI. Reactions with interhalogens (IX; X = Cl, Br) afford the respective mixed halides ($4\text{-}RC_6H_4$)(SB)TeIX, which tend to disproportionate in solution on standing. Surprisingly, the pseudo halogen, thiocyanogen failed to react with **1a**–**c** at room temperature.

Presence of the 1,4-Te···N coordinative interaction (vide infra) in hybrid tellurides **1a**–**c** is also expected to enhance (at least marginally) the electron density at the Te center. Reactions of **1a**–**c** were therefore, carried out with Pt(II) and Hg(II) halides. Reactions with mercury halides afforded the pale orange crystalline adducts HgX$_2$[$4\text{-}RC_6H_4$(SB)Te]$_2$, **2a**–**c** (X = Cl) and **3a**–**c** (X = Br) but PtCl$_2$(PhCN)$_2$ failed to react in refluxing chloroform. Attempts to prepare the 1:1 adduct by reacting equimolar quantities of **1a**–**c** and HgCl$_2$ failed, producing only **2a**–**c** and unreacted HgCl$_2$. This is interesting as most of the tellurides either afford 1:1 adduct or both 1:1 and 1:2 adducts with HgX$_2$. Even heating of the adducts **2**, **3** in refluxing chloroform does not lead to cleavage of Te–C bond as reported in case of adducts formed by tellurides that involve 1,5-Te···N(O) intramolecular interactions. It appears that the σ-donor strength of the tellurides **1** is better than the halide resulting in the formation of 1:2 adducts instead of 1:1, which invariably involve bridging halide ligands. However, quantitative displacement of **1c** from **3c** by PPh$_3$, clearly suggests that the tertiary phosphine (pK_a 2.73) [10] is a stronger donor than the telluride ligands. Such a displacement reaction thereby provides a route to purify the tellurides, at least in case of **1**. The IR spectrum of **2c** contains a sharp signal corresponding to C=N at 1610.3 wave number, which is somewhat higher than that in the telluride **1c** (1586.5). There is little change in the methine ^{1}H NMR chemical shift between tellurides and the mercury adducts. The solution ^{125}Te NMR spectra of **2a**–**c** and **3a**–**c** show a single resonance which are slightly more shielded (by between 16 and 31 ppm) than the tellurides **1a**–**c**. Solid-state ^{125}Te CP MAS NMR of **2a** shows two isotropic shifts at 438 and 467 ppm, which is consistent with the crystal structure (vide infra). Only one isotropic shift is observed for **2c** at 417 ppm, indicating that the two tellurium atoms are symmetry related, as in the crystal structure of the bromine analogue, **3c**. For both **2a** and **2c**, the solid-state ^{125}Te NMR signals are shifted by between 105 and 134 ppm to lower frequency than the solution state signals, most likely as a result of the presence of intermolecular interactions in the solid-state.

2.1. Crystal structures of **1b** and **1c**

ORTEP diagrams of the molecular structures of **1b** and **1c** are shown in Fig. 1 and the relevant bond parameters included in Table 3. The Te–C bond lengths and the included angle in **1b** and **1c** are characteristic of diaryltellurides and their solid-state molecular structures are almost superimposable, differing only in the orientation of the nitro-substituted benzene ring. An interesting feature of the molecular structures of these tellurides is the presence of a 1,4-type intramolecular SBI between Te and the imine N atoms. The fact that the Te···N distance (2.924(4) Å in **1b**, 3.107(4) Å in **1c**) is smaller than the sum of their van der Waals radii (3.61 Å) is not a mere geometrical consequence.[1] The attractive interaction between Te(II) and the *ortho* substituted azomethine nitrogen atom becomes obvious from the bending of N1–C2 and Te–C1 bonds towards each other resulting in the appreciable angular distortions in Te–C1–C2 and N1–C2–C1 bond angles that are reduced to 114.2(3), 113.9(3)° in **1b** and 116.0(3), 117.5(3)° in **1c** compared to the ideal value of 120°. The Te–C15 bond *trans* to Te···N is also coplanar with the four-membered heterocyclic ring (distance of C15 from the Te, C1, C2, N1 mean plane is 0.0671 Å in **1b**, 0.1166 Å in **1c**), although the C15–Te···N1 angle is far from being linear (149.8(1)° in **1b**, 145.5(1)° in **1c**). In the diorganotellurium compounds involving 1,5-Te···N/O SBIs, coplanarity of the *trans* Te–C bond with the heterocyclic ring has invariably been

---

[1] Te···N1 distance calculated from the observed Te–C1, C1–C2, C2–N1 bond lengths and assuming bond angles Te–C1–C2 and N1–C2–C1 each to be 120° is 3.18 Å in **1b** and 3.23 Å in **1c**.

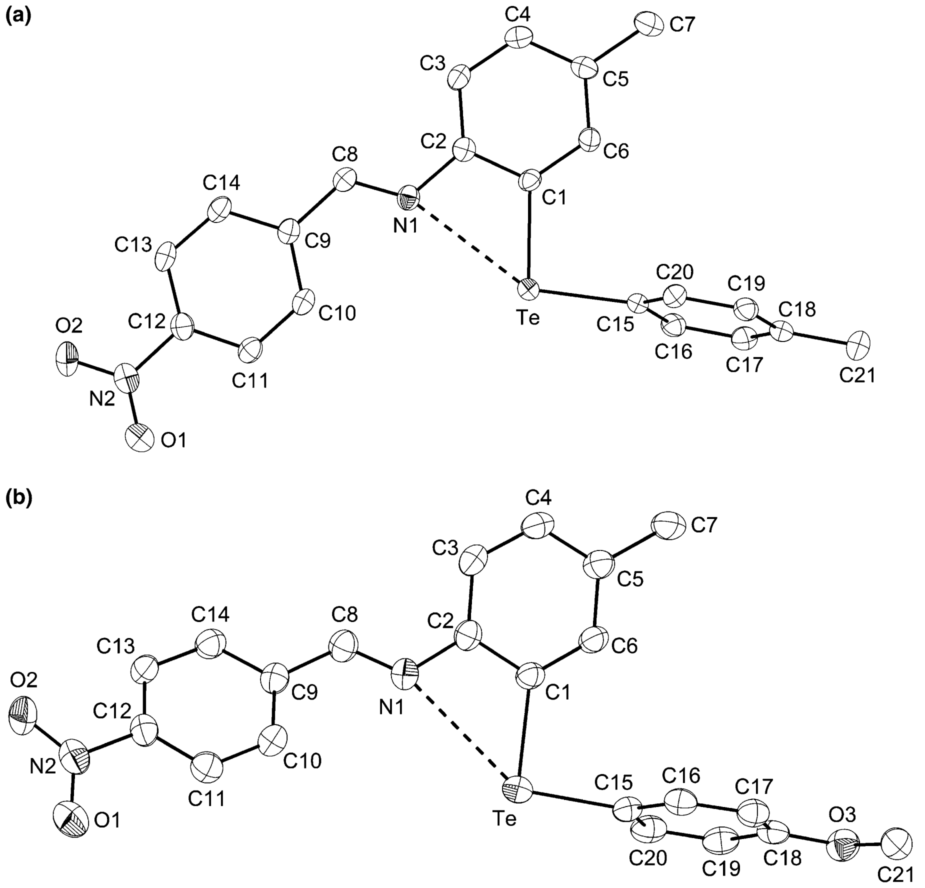

Fig. 1. Molecular structures showing 50% probability displacement ellipsoids and the crystallographic numbering scheme (a) **1b** and (b) **1c**.

Table 3
Selected bond parameters (Å, °) for **1b**, **1c**, **2a** and **3c**

	1b	**1c**	**2a**		**3c**	
			X = A	X = B		
Hg–TeX			2.800(1)	2.773(1)	Hg–Te	2.797(3)
Hg–ClX			2.496(2)	2.457(2)	Hg–Br	2.656(2)
Te1–N1	2.924(4)	3.106(4)	2.898(7)	2.959(7)	Te1–N1	2.941(4)
Te1–C1	2.122(4)	2.144(5)	2.125(8)	2.102(8)	Te1–C1	2.110(4)
Te1–C15	2.132(4)	2.148(5)	2.104(8)	2.098(8)	Te1–C15	2.114(4)
N1–C2	1.425(5)	1.430(6)	1.41(1)	1.41(1)	N1–C2	1.411(5)
N1–C8	1.281(5)	1.292(6)	1.26(1)	1.27(1)	N1–C8	1.274(5)
C1–C2	1.406(6)	1.437(5)	1.40(1)	1.39(1)	C1–C2	1.402(5)
TeA–Hg–TeB			108.67(2)		Te–Hg–Te^{i}	137.29(1)
TeX–Hg–ClA			100.58(5)	117.14(5)	Te–Hg–Br	91.80(1)
TeX–Hg–ClB			116.09(5)	106.54(5)	Te–Hg–Br^{i}	110.59(1)
ClA–Hg–ClB			108.19(7)		Br–Hg–Br^{i}	116.53(1)
Hg–Te–N1			78.9(1)	88.5(1)	Hg–Te–N1	85.32(6)
Hg–Te–C1			94.3(2)	95.5(2)	Hg–Te–C1	108.12(9)
Hg–Te–C15			102.0(2)	99.2(2)	Hg–Te–C15	102.9(1)
N1–Te–C1	53.3(1)	51.8(1)	53.9(3)	52.7(3)	N1–Te–C1	52.9(1)
N1–Te–C15	149.8(1)	145.5(1)	150.0(2)	149.1(2)	N1–Te–C15	147.8(1)
C1–Te–C15	96.5(2)	93.9(1)	96.4(3)	96.6(3)	C1–Te–C15	95.2 (1)
Te–N1–C2	78.6(2)	74.8(2)	78.2(4)	76.8(4)	Te–N1–C2	77.6(2)
Te–N1–C8	158.6(3)	147.5(3)	145.6(6)	151.3(6)	Te–N1–C8	161.1(3)
C2–N1–C8	122.5(3)	118.8(4)	120.1(7)	119.8(7)	C2–N1–C8	119.8(3)

Symmetry operation used to generate equivalent atoms: (i) $-x, y, -0.5 - z$.

observed and the C–Te···N/O triad is reported to attain an almost linear alignment (C–Te···N/O angles fall in the range 157–170°). Coplanarity of the C15–Te bond with the N1–C2–C1–Te plane in **1b** and**1c** makes $n_N \rightarrow \sigma^*_{(Te–C)}$ interaction feasible but due to non-linearity of N···Te–C15 triad, the orbital overlap is insufficient to cause Te–C bond cleavage upon interaction with mercury(II) halides. Such SBIs, however, contribute to the overall stability of low valent compounds of chalcogens as has been inferred from ab initio MO and DFT calculations on intramolecular 1,4-type non-bonded interactions between oxygen and chalcogen elements [11]. Similar 1,4-Te···N intramolecular SBIs among the other structurally characterized diorganotellurides with more flexible ethylene spacers between tellurium and nitrogen was either absent or not looked into [12].

The crystal structures of **1b** and **1c** are devoid of any intermolecular SBIs involving Te(II), which appears to be due to the reduced Lewis acidity of tellurium center (as compared to the corresponding Te(IV) dihalides [8]) as well as its involvement in the intramolecular Te···N interaction. The supramolecular architecture in the crystalline phase of **1b** formed under self-assembly conditions represents a fascinating case of molecular tectonic approach [13] of crystal engineering. Each molecule behaves as a multipoint self-complimentary tecton (Chart 1, A) and the topological properties of intermolecular reciprocatory C13–H13···O2 interaction results in the formation of zero-dimensional centrosymmetric dimers as the supramolecular synthon (Chart 1, B) which is common among the organic molecular crystals [14]. The other C19–H19···O1 H-bond in cooperation with the C8–H8···π(CH=N) interaction organizes these synthons into an extended array that bears a centre of inversion. The C11–H11···π(aryl) interactions then weave these double stranded molecular chains into a three-dimensional supramolecular motif (Fig. 2). In **1c**, on the other hand, interactions between the more acidic methyl protons and π-electron density of Te-substituted benzene ring or that of azomethine bond (methoxy)C–H···π (Te substituted C_6H_3/CH=N) appears to be the only molecular associative forces responsible for the observed crystal lattice. As the chances of forming a dimer using this particular interaction in a reciprocal manner appear limited the observed catemer seems to be the energetically favored choice. The overall packing of molecules in both the tellurides conforms to the centrosymmetric space groups $P2_1/n$ and $P2_1/c$, respectively. Consequently, all putative second-order NLO effects (reported for the monoclinic modification of NMBA, space group *Pc*) are nullified in case of **1b** and **1c** which precludes their application as NLO materials.

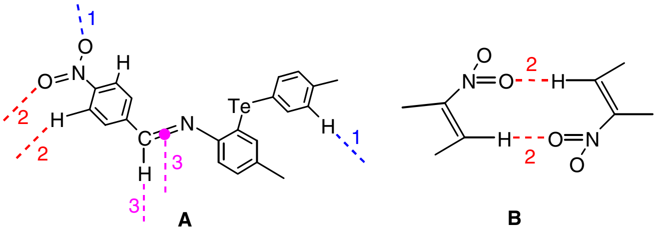

Chart 1.

2.2. Crystal structures of 2a and 3c

ORTEP diagrams of the molecular structures of **2a** and **3c** are shown in Fig. 3 and the relevant bond parameters included in Table 3. The geometry of the HgX_2Te_2 units in these complexes is distorted tetrahedral. The angular distortion around the central Hg(II) atom in **2a** is limited over a small range, 100.16(5)–117.11(5)° and values of the bond angles Cl–Hg–Cl, 108.19(7)° and Te–Hg–Te, 108.67(2)° are close to the ideal tetrahedral value. The observed Hg–Cl and Hg–Te bond lengths are comparable

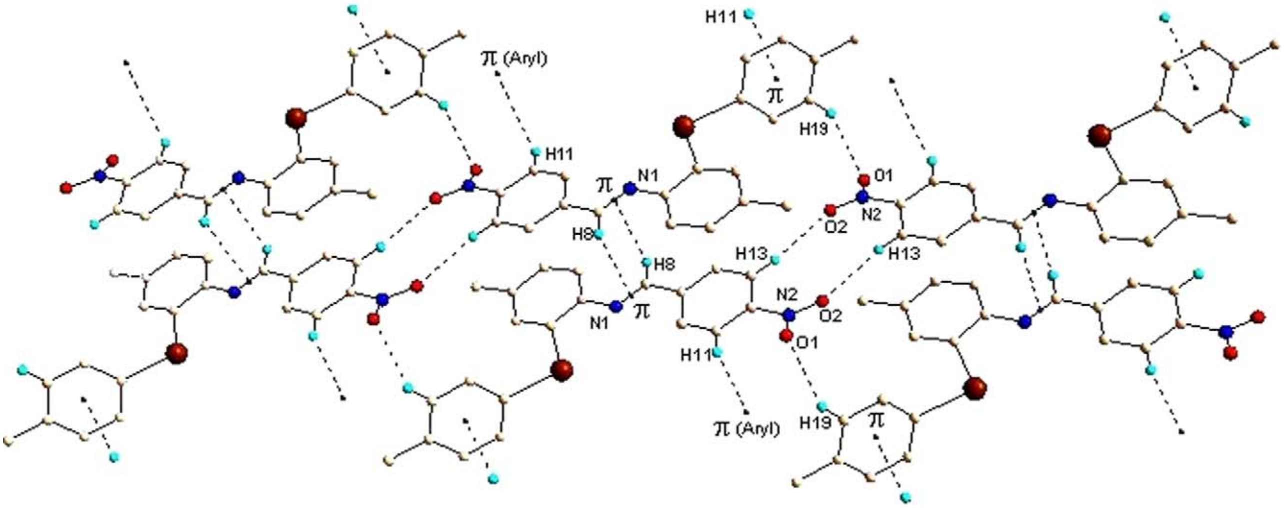

Fig. 2. View of the 1D Chain of 4-MeC_6H_4(SB)Te (**1b**) consisting of a pair of anti-parallel rows of molecules via C–H···O and C–H···π interactions.

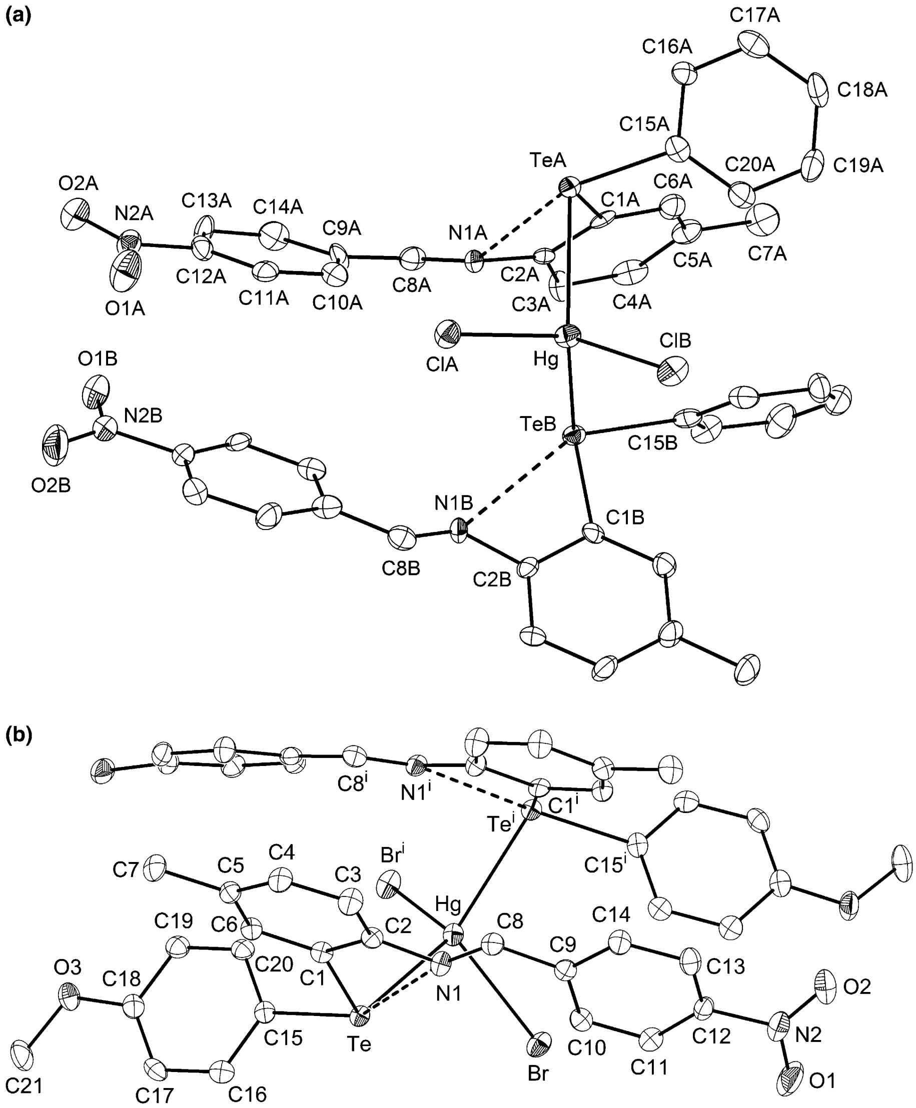

Fig. 3. Molecular structures showing 50% probability displacement ellipsoids and the crystallographic numbering scheme (a) **2a** and (b) **3c**.

to the corresponding values reported for the $HgCl_2$ complex of chelating bis(telluride), 1,6-bis(2-butyltellurophenyl)-2,5-diazahexa-1,5-diene [15]. The $HgBr_2Te_2$ unit in **3c** comprises of two symmetry related ($i = -x, y, -0.5 - z$) halves with Hg–Br and Hg–Te bond distances of 2.656(2) and 2.797(3) Å, respectively. Steric bulk of the Br atoms in this complex, however, causes greater repulsion among electron rich ligands and distorts the coordination tetrahedron of the mercury atom considerably, resulting in a Te–Hg–Te^{i} angle as large as 137.29(1)°. Almost similar values for Hg–Te bond lengths in the two independent molecules of **2b** as well as in **3c** indicate insignificant role of the electronic factor of halogen atoms attached to Hg(II) on its geometry. The observed difference in the orientation of the ligand atoms around the central mercury atoms in the two complexes (**2a** and **3c**) could be a manifestation of steric bulk of X ligands together with the variation of nature and strength of intermolecular SBIs in the solid-state.

It has been recognized that M–Cl moieties are good anisotropic H-bond acceptors. The acceptor strength of metal-bound Cl atoms towards O–H, N–H [16] and C–H [17] donors parallels that of Cl^- anion and the directionality and predictability of intermolecular $C–H\cdots Cl_{(2-3)}–M$ interactions have been compared with coordinative covalent interactions [18]. The crystal packings in the neutral complexes **2a** and **3c** have, therefore, been analyzed to ascertain the role of mercury-bound halogen atoms, if any, in the formation of supramolecular motifs via weak $C–H\cdots X$ interactions. While the $C4A–H4A\cdots Cl1B$ interaction in **2a** arrange the identically oriented molecules in a row, the other reciprocal $C8A–H8B\cdots Cl1A$ interaction connects two such *anti*-parallel rows to form zero-dimensional dimers with a center of inversion between symmetry related molecules from the two rows. The intermolecular $C–H\cdots O$(nitro) interactions link these extended arrays into three-dimensional motifs.

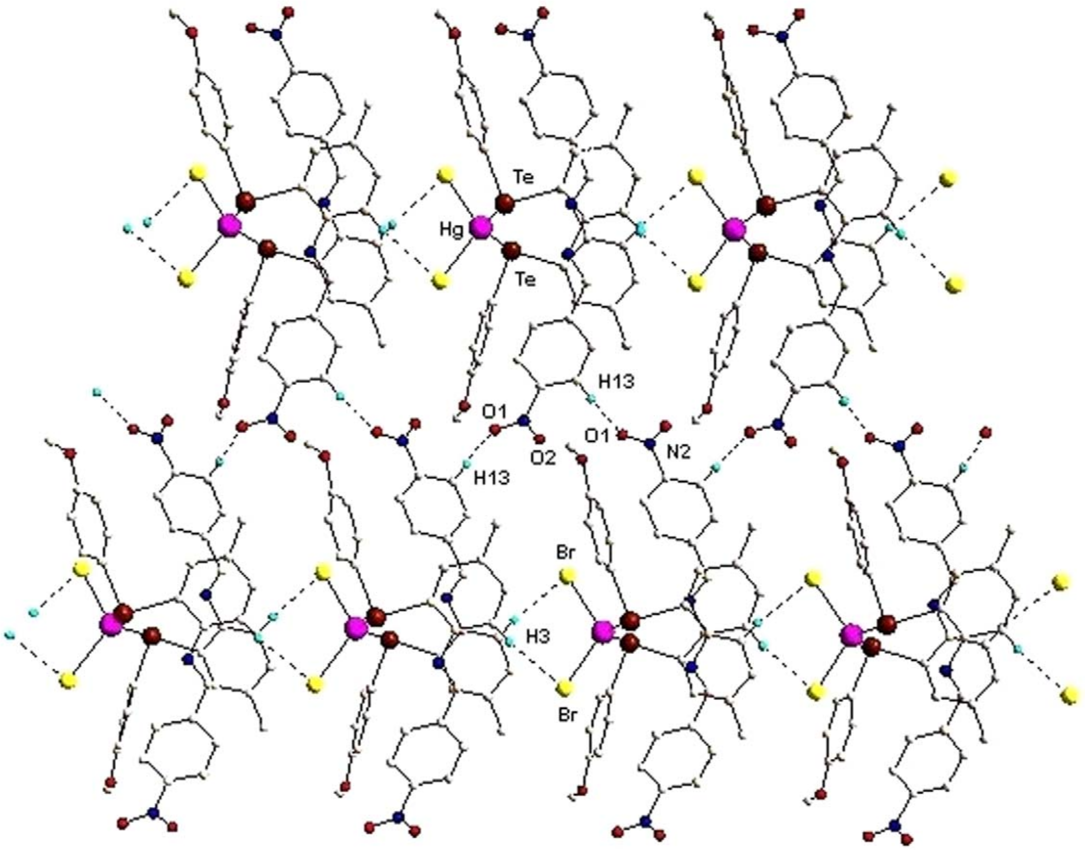

Fig. 4. View of the 1D supramolecular motif comprising of C–H· · ·O interlinked pair of rows which are formed by a combination of coordinative Hg–Te and C3–H3· · ·Br interactions of $[4\text{-MeOC}_6H_4(SB)Te]_2HgBr_2$ (**3c**).

The role of mercury bound bromine atoms in the formation of supramolecular structure in the crystal lattice of **3c** is equally important in context of recent strategies to combine analogous C–H· · ·Cl–M interaction with transition metal coordination chemistry to create metal containing supramolecular synthons for the molecular recognition in the area of inorganic crystal engineering [19,20]. The C–H· · ·Br intermolecular interaction in **3c** appear to possess the desired directionality and significance for supramolecular architecture. The one-dimensional supramolecular motif formed by a balanced combination of coordinative covalent (Hg–Te) and (C3–H3· · ·Br) SBIs in **3c** (Fig. 4) may be compared with the 1D directional coordination network based upon self-assembly of a bridging ligand and metal halide [21].

2.3. Conclusions

The tellurides **1** possess rare intramolecular 1,4-Te· · ·N interaction which is retained and does not lead to Te–C bond cleavage upon coordination to mercury(II) halides as observed earlier for some 1,5-Te· · ·N(O) containing tellurides. Complete displacement of **1** from adducts **2** by PPh_3, though not very surprising, is of interest as a route to purify **1**. The crystal packings of tellurides, **1b** and **1c**, illustrate the dominance of C–H· · ·O/C–H· · ·π interactions over SBIs involving Te in the formation of supramolecular synthons. Identification of metal assisted C–H· · ·X–M interactions in the crystal lattice of **2a** and **3c**, indicates that these interactions, though weak in strength, possess the desired directionality and predictability. Such observations may be useful in designing the building blocks for crystal engineering so as to achieve the dream of rationally constructing functionalized supramolecular architecture in molecular solids, which is still a daunting task.

3. Experimental

3.1. Material and instruments

The organotellurium halides, $4\text{-RC}_6H_4(SB)TeCl_2$, were prepared by transmetallation reactions between (SB)HgCl and $4\text{-RC}_6H_4TeCl_3$, as reported earlier [8]. IBr and $(SCN)_2$ were prepared by literature methods whereas iodine monochloride and methyl iodide were procured from Merck (Germany) and were distilled before use. Melting points were recorded in capillary tubes and are uncorrected. ^{1}H NMR spectra were recorded at 300.13 MHz in $CDCl_3$ on a Varian DRX 300 Spectrometer using TMS as internal standard. Solution ^{13}C (100.54 MHz) and ^{125}Te (126.19 MHz) NMR spectra were recorded in d_6-DMSO on a JEOL Eclipse Plus 400 NMR spectrometer, using Me_4Si and Me_2Te as internal standards. Solid-state ^{125}Te (126.19 MHz) CP MAS NMR spectra were acquired on the same instrument with a 6 mm MAS probe operating at spinning frequencies between 5 and 10 KHz. Experimental condition: 1 μs pulse width, 5 s relaxation delay, 10000 transients. The isotropic chemical shifts are referenced against Me_2Te using solid $Te(OH)_6$ as the secondary reference (δ_{iso} 692.1, 685.5) [22]. IR spectra were examined as KBr pellets using a Perkin–Elmer RX1 Spectrometer. Elemental carbon, hydrogen and nitrogen analyses were performed on a Carlo Erba 1108 make analyzer. Tellurium was estimated volumetrically and the halogen content gravimetrically as silver halide.

3.2. Synthesis

3.2.1. Reduction reactions

*3.2.1.1. Synthesis of 4-$MeOC_6H_4(SB)Te$ (**1c**).* A solution of 4-$MeOC_6H_4(SB)TeCl_2$ (1.09 g, 2 mmol) in dichloromethane (50 mL) was shaken with an aqueous solution of $Na_2S_2O_5$ (0.57 g, 3 mmol) for 15 min. The organic layer gradually turned reddish orange. It was separated, washed (4 × 50 mL) with water and dried over anhydrous Na_2SO_4 overnight. Volatiles were removed under reduced pressure and the residue was crystallized from chloroform/diethyl ether to give red rhombus crystals of **1c**. Yield: 0.7 g, 74%. M.p.: 120 °C. Anal. Calc. for $C_{21}H_{18}N_2O_3Te$: C, 53.21; H, 3.83; N, 5.91; Te, 26.92. Found: C, 53.00; H, 3.96; N, 6.05; Te, 26.10%. IR (KBr, cm^{-1}): 1586.5 (CH=N). ^{1}H NMR (300.13 MHz, $CDCl_3$, 25 °C): δ 2.19 (s, 3H, CH_3), 3.86 (s, 3H, OCH_3), 6.78–8.35 (m, 11H, Arom), 8.55 (s, 1H, CH=N).

*3.2.1.2. Synthesis of 4-$MeC_6H_4(SB)Te$ (**1b**).* A solution of 4-$MeC_6H_4(SB)TeCl_2$ (1.06 g, 2 mmol) in chloroform and $Na_2S_2O_5$ (0.57 g, 3 mmol) in water gave red crystals of **1b** by following the same procedure as in **1.1**. Yield: 0.6 g, 66%. M.p.: 140 °C. Anal. Calc. for $C_{21}H_{18}N_2O_2Te$: C, 57.07; H, 3.96; N, 6.12; Te, 27.86. Found: C, 56.90; H, 4.09; N, 6.37; Te, 27.00%. IR (KBr, cm^{-1}): 1586.5 (CH=N). ^{1}H NMR (300.13 MHz, $CDCl_3$, 25 °C): δ 2.34 (s, 3H, CH_3), 2.50 (s, 3H, CH_3), 7.39–8.39 (m, 11H, Arom), 8.87 (s, 1H, CH=N).

*3.2.1.3. Synthesis of $Ph(SB)Te$ (**1a**).* Compound $Ph(SB)TeCl_2$ (0.9 g, 2 mmol) and $Na_2S_2O_5$ (twofold) were shaken in two phase solvent system (CH_2Cl_2/H_2O) for 5 min. The organic layer slightly turned orange. It was separated and washed (2 × 50 mL) with water. It was again treated with $Na_2S_2O_5$ thrice successively (single step reduction was avoided to prevent decomposition). The organic layer was finely separated and dried over anhydrous Na_2SO_4 for 1 h. The reaction mixture was concentrated under reduced pressure and the residue was crystallized from chloroform/petroleum ether to give red crystals of **1a**. Yield: 0.55 g, 62%. M.p.: 118 °C. Anal. Calc. for $C_{20}H_{16}N_2O_2Te$: C, 54.11; H, 3.63; N, 6.31; Te, 28.74. Found: C, 54.30; H, 3.52; N, 6.12; Te, 28.53%. IR (KBr, cm^{-1}): 1590.2 (CH=N). ^{1}H NMR (300.13 MHz, $CDCl_3$, 25 °C): δ 2.40 (s, 3H, CH_3), 7.23–8.37 (m, 12H, Arom), 8.75 (s, 1H, CH=N).

*3.2.2. Reaction of tellurides, **1** with HgX_2 (X = Cl, Br)*

*3.2.2.1. $[4\text{-}MeOC_6H_4(SB)Te]_2HgCl_2$ (**2c**).* To a solution of **1c** (1.9 g, 4 mmol) in acetonitrile (100 mL), mercury(II) chloride (0.54 g, 2 mmol) in the same solvent (50 mL) was added slowly. A yellow solid gradually separated during the addition. After stirring for 3 h the solid was filtered, washed with acetonitrile and dried. Light yellow solid was recrystallized from DMF to give orange yellow needles of **2c**. Yield: 2.17 g, 89%. M.p.: 222 °C. Anal. Calc. for $C_{42}H_{36}N_4O_6Cl_2HgTe_2$: C, 41.37; H, 2.98; N, 4.59; Te, 20.93. Found: C, 41.50; H, 3.02; N, 4.40; Te, 20.21%. IR (KBr, cm^{-1}): 1610.3 (νH=N). ^{1}H NMR (300.13 MHz, $CDCl_3$, 25 °C): δ 2.20 (s, 6H, $2CH_3$), 3.87 (s, 6H, $2OCH_3$), 6.81–8.36 (m, 22H, Arom), 8.57 (s, 2H, 2CH=N).

The following adducts were prepared similarly.

*3.2.2.2. $[4\text{-}MeC_6H_4(SB)Te]_2HgCl_2$ (**2b**).* Yield: 91%. M.p.: 228 °C. Anal. Calc. for $C_{42}H_{36}N_4O_4Cl_2HgTe_2$: C, 42.48; H, 3.06; N, 4.72; Te, 21.49. Found: C, 42.30; H, 3.11; N, 4.59; Te, 22.00%. ^{1}H NMR (300.13 MHz, $CDCl_3$, 25 °C): δ 2.22 (s, 6H, $2CH_3$), 2.42 (s, 6H, $2CH_3$), 6.87–8.35 (m, 22H, Arom), 8.56 (s, 2H, 2CH=N).

*3.2.2.3. $[Ph(SB)Te]_2HgCl_2$ (**2a**).* Yield: 78%. M.p.: 240 °C. Anal. Calc. for $C_{40}H_{32}N_4O_4Cl_2HgTe_2$: C, 41.44; H, 2.78; N, 4.83; Te, 22.01. Found: C, 41.90; H, 2.60; N, 4.92; Te, 22.02%. ^{1}H NMR (300.13 MHz, $CDCl_3$, 25 °C): δ 2.21 (s, 6H, $2CH_3$), 6.87–8.34 (m, 24H, Arom), 8.58 (s, 2H, 2CH=N).

*3.2.2.4. $[4\text{-}MeOC_6H_4(SB)Te]_2HgBr_2$ (**3c**).* Yield: 2.17 g, 82%. M.p.: 220 °C. Anal. Calc. for $C_{42}H_{36}N_4O_6Br_2HgTe_2$: C, 38.56; H, 2.77; N, 4.28; Te, 19.51. Found: C, 38.22; H, 2.59; N, 4.56; Te, 20.20%. ^{1}H NMR (300.13 MHz, $CDCl_3$, 25 °C): δ 2.96 (s, 6H, $2CH_3$), 3.87 (s, 6H, $2OCH_3$), 6.79–8.36 (m, 22H, Arom), 8.57 (s, 2H, CH=N).

*3.2.2.5. $[4\text{-}MeC_6H_4(SB)Te]_2HgBr_2$ (**3b**).* Yield: 87%. M.p.: 235 °C. Anal. Calc. for $C_{42}H_{36}N_4O_4Br_2HgTe_2$: C, 39.52; H, 2.84; N, 4.39; Te, 19.99. Found: C, 39.80; H, 2.99; N, 4.28; Te, 19.67%. ^{1}H NMR (300.13 MHz, $CDCl_3$, 25 °C): δ 2.21 (s, 6H, $2CH_3$), 2.23 (s, 6H, $2CH_3$), 6.83–8.30 (m, 22H, Arom), 8.49 (s, 2H, CH=N).

*3.2.2.6. $[Ph(SB)Te]_2HgBr_2$ (**3a**).* Yield: 91%. M.p.: 236 °C. Anal. Calc. for $C_{40}H_{32}N_4O_4Br_2HgTe_2$: C, 38.49; H, 2.58; N, 4.49; Te, 20.44. Found: C, 38.22; H, 2.69; N, 4.68; Te, 20.90%. ^{1}H NMR (300.13 MHz, $CDCl_3$, 25 °C): δ 2.23 (s, 6H, $2CH_3$), 6.86–8.32 (m, 24H, Arom), 8.59 (s, 2H, CH=N).

3.2.2.7. Attempted preparation of 1:1 adduct. Mercury(II) chloride (1.08 g, 4 mmol) in acetonitrile (∼80 mL) was added slowly to a solution of **1c** (1.9 g, 4 mmol) in acetonitrile (∼100 mL). A light yellow solid gradually separated during the addition. After stirring for 3 h the solid was filtered, washed with acetonitrile and dried. It was found to be **2c**. The filtrate on concentration afforded unreacted $HgCl_2$ (0.5 g).

3.2.3. Oxidative addition reactions of 1

*3.2.3.1. Synthesis of 4-MeOC$_6$H$_4$(SB)TeBr$_2$: **1c**.* (0.47 g, 1 mmol) was dissolved in carbon tetrachloride (20 mL) and a solution of bromine (0.18 mL, 1.2 mmol) in the same solvent was slowly added with stirring. A light yellow colored solid separated which was filtered, dried and recrystallized with $CHCl_3$ to give 4-MeOC$_6$H$_4$(SB)TeBr$_2$. Yield: 0.52 g, 82%. M.p.: 180 °C (lit [8], 180 °C). Anal. Calc. for $C_{21}H_{18}N_2O_3Br_2Te$: C, 39.80; H, 2.86; N, 4.42; Br, 25.21; Te, 20.13. Found: C, 39.73; H, 2.64; N, 4.60; Br, 24.10; Te, 21.07%. IR (KBr, cm^{-1}): 1583.08 (CH=N). ^{1}H NMR (300.13 MHz, $CDCl_3$, 25 °C): δ 2.36 (s, 3H, CH_3), 3.94 (s, 3H, OCH_3), 7.15–8.41 (m, 11H, Arom), 8.89 (s, 1H, CH=N).

3.2.3.2. Synthesis of 4-MeOC$_6$H$_4$(SB)TeI$_2$. Iodine (0.26 g, 1 mmol) in carbon tetrachloride (10 mL) was added dropwise to a solution of **1c** (0.47 g, 1 mmol) in carbon tetrachloride (10 mL) with stirring. A dark solid gradually formed which after 0.5 h, was collected by filtration, washed with pet ether and characterized as 4-MeOC$_6$H$_4$(SB)TeI$_2$. Yield: 0.63 g, 86%. M.p.: 196 °C (lit [8], 196 °C). Anal. Calc. for $C_{21}H_{18}N_2O_3I_2Te$: C, 34.66; H, 2.49; N, 3.85; I, 34.87; Te, 17.53. Found: C, 34.88; H, 2.54; N, 4.03; I, 34.52; Te, 17.07%.

3.2.3.3. Synthesis of 4-MeOC$_6$H$_4$(SB)TeICl. To the solution of **1c** (0.47 g, 1 mmol) in carbon tetrachloride (20 mL) was added a solution of iodine monochloride (0.81 g, 1.1 mmol) in carbon tetrachloride with stirring at room temperature. A light yellow colored solid was obtained which was filtered, washed with carbon tetrachloride and recrystallized from chloroform to give yellow needles of 4-MeOC$_6$H$_4$(SB)TeICl. Yield: 0.44 g, 59%. M.p.: 216 °C. Anal. Calc. for $C_{21}H_{18}N_2O_3IClTe$: C, 39.64; H, 2.85; N, 4.40; ICl, 25.51; Te, 20.05. Found: C, 39.62; H, 2.69; N, 4.46; ICl, 26.03; Te, 21.07%. IR (KBr, cm^{-1}): 1593.5 (CH=N). ^{1}H NMR (300.13 MHz, $CDCl_3$, 25 °C): δ 2.34 (s, 3H, CH_3), 3.92 (s, 3H, OCH_3), 7.15–8.35 (m, 11H, Arom), 8.87 (s, 1H, CH=N). ^{13}C NMR: δ 21.54, 55.61, 114.15, 116.46, 118.71, 124.27, 130.52, 130.09, 133.82, 137.30, 144.21, 156.60, 162.38. ^{125}Te NMR: δ 884.8 ppm.

Table 4
Crystal data and structure refinement for **1b**, **1c**, **2a** and **3c**

	1b	**1c**	**2a**	**3c**
Formula	$C_{21}H_{18}N_2O_2Te$	$C_{21}H_{18}N_2O_3Te$	$C_{40}H_{32}Cl_2HgN_4O_4Te_2$	$C_{42}H_{36}Br_2HgN_4O_6Te_2$
Formula weight (g mol^{-1})	457.97	473.97	1159.39	1308.36
Crystal system	Monoclinic	Monoclinic	Monoclinic	Monoclinic
Crystal size (mm)	0.10 × 0.45 × 0.85	0.10 × 0.65 × 0.95	0.08 × 0.18 × 0.52	0.25 × 0.50 × 0.75
Space group	$P2_1/n$	$P2_1/c$	$P2_1/n$	$C2/c$
a (Å)	7.318(1)	9.1659(14)	15.334(2)	30.254(6)
b (Å)	13.558(3)	22.191(3)	9.166(2)	9.324(2)
c (Å)	19.370(4)	9.8526(15)	28.156(1)	14.926(3)
α (°)	90	90	90	90
β (°)	96.686(3)	99.803(3)	92.077(1)	97.844(3)
γ (°)	90	90	90	90
V (Å^3)	1908.7(6)	1974.8(5)	3954.7(10)	4171.3(13)
Z	4	4	4	4
D_{calcd} (Mg m^{-3})	1.594	1.594	1.947	2.083
T (K)	103(2)	148(2)	93(2)	103(2)
μ (mm^{-1})	1.575	1.529	5.519	7.029
$F(000)$	904	936	2200	2472
θ Range (°)	2.2–27.5	2.2–27.5	1.4–27.5	2.3–27.5
Index ranges	$-8 \leqslant k \leqslant 9$; $-16 \leqslant l \leqslant 17$; $-23 \leqslant h \leqslant 25$	$-11 \leqslant k \leqslant 11$; $-28 \leqslant l \leqslant 25$; $-12 \leqslant h \leqslant 12$	$-19 \leqslant k \leqslant 19$; $0 \leqslant l \leqslant 11$; $0 \leqslant h \leqslant 36$	$-39 \leqslant k \leqslant 35$; $-12 \leqslant l \leqslant 11$; $-19 \leqslant h \leqslant 18$
Number of reflections collected	13127	14217	12124	14604
Completeness to θ_{max} (%)	99.4	99.6	99.8	99.5
Number of independent reflections/R_{int}	4355	4510	12124	4765
Number of reflection observed with ($I > 2\sigma(I)$)	3356	4077	10246	4461
Number of refined parameters	235	244	480	259
GOF (F^2)	1.053	1.198	1.091	1.056
R_1 (F) ($I > 2\sigma(I)$)	0.038	0.046	0.058	0.030
wR_2 (F^2) (all Data)	0.094	0.108	0.157	0.073
$(\Delta/\sigma)_{max}$	<0.0001	<0.0001	0.0009(1)	<0.0061(5)
Largest difference in peak/hole (e Å^{-3})	1.708/−0.697	0.799/−1.174	2.157 (near Hg)/−1.491 (near Hg)	2.812 (near Hg)/−2.486 (near Hg)

3.2.3.4. Synthesis of 4-MeOC$_6$H$_4$(SB)TeIBr. A freshly prepared solution of iodine monobromide (0.21 g, 1.1 mmol) in carbon tetrachloride was slowly added to the solution of **1c** (0.47 g, 1 mmol) in the same solvent. Orange red product separated during addition. It was filtered, washed with carbon tetrachloride and recrystallized with $CHCl_3$ to give 4-MeOC$_6$H$_4$(SB)TeIBr. Yield: 0.43 g, 63%. M.p.: 190 °C. Anal. Calc. for $C_{21}H_{18}N_2O_3IBrTe$: C, 37.05; H, 2.66; N, 4.11; IBr, 30.38; Te, 18.74. Found: C, 36.86; H, 2.54; N, 4.09; IBr, 31.03; Te, 18.07%. IR (KBr, cm^{-1}): 1598.6 (CH=N). ^{1}H NMR (300.13 MHz, CDCl$_3$, 25 °C): δ 2.38 (s, 3H, CH$_3$), 3.93 (s, 3H, OCH$_3$), 7.01–8.43 (m, 11H, Arom), 8.89 (s, 1H, CH=N). ^{13}C NMR: δ 21.53, 55.58, 115.98, 116.69, 124.30, 130.15, 131.72, 133.81, 140.41, 144.15, 156.24, 162.20. ^{125}Te NMR: δ 841.9 ppm.

3.2.4. Synthesis of 4-MeOC$_6$H$_4$(SB)TeCl$_2$

To a solution of **1c** (0.47 g, 1 mmol) in carbon tetrachloride (30 mL), sulfuryl chloride (0.5 mL) was added dropwise with stirring at 0 °C. The reaction mixture was allowed to come to the room temperature and stirred for 15 min. Concentration under reduced pressure and addition of pet-ether afforded the colorless crystalline 4-MeOC$_6$H$_4$(SB)TeCl$_2$. Yield: 0.42 g, 70%.

4-MeC$_6$H$_4$(SB)TeCl$_2$ and Ph(SB)TeCl$_2$ were prepared similarly from **1b** and **1a**, respectively, in 70–75% yield. All these dichlorides, 4-RC$_6$H$_4$(SB)TeCl$_2$ were authenticated by their melting points and IR spectra [8].

*Reaction of **3c** with Ph$_3$P.* To a suspension of **3c** (1.3 g, 1 mmol) in acetonitrile (20 mL) was added dropwise a solution of Ph$_3$P (0.53 g, 2 mmol) in the same solvent at room temperature. The reaction mixture changed to a dark red suspension. It was filtered to remove the $(Ph_3P)_2HgBr_2$ complex and washed with ether. The dark red filtrate on concentration afforded **1c** in quantitative yield (0.87 g, 1.9 mmol).

3.3. Crystallography

Single crystals of **1b**, **1c**, **2a** and **3c** suitable for X-ray crystallography were obtained by slow evaporation of chloroform solutions. Intensity data were collected on a Bruker PS4 diffractometer with graphite-monochromated Mo Kα (0.7107 Å) radiation. Data were reduced and corrected for absorption using the programs SAINT and SADABS [23]. The structures were solved by direct methods and difference Fourier synthesis using SHELXS-97 implemented in the program WINGX 2002 [24]. Full-matrix least-squares refinements on F^2, using all data, were carried out with anisotropic displacement parameters applied to all non-hydrogen atoms. Hydrogen atoms were included in geometrically calculated positions using a riding model and were refined isotropically. Crystallographic parameters and details of the data collection and refinement are given in Table 4. Figures were created using DIAMOND [25].

4. Supplementary material

Crystallographic data (excluding structure factors) for the structural analyses have been deposited with the Cambridge Crystallographic Data Centre, CCDC Nos. 289963 (**1b**), 246744 (**1c**), 289962 (**2a**) and 289961 (**3c**) (Supporting Information). Copies of this information may be obtained free of charge from The Director, CCDC, 12 Union Road, Cambridge CB2 1EZ, UK (fax: +44 1223 336 033; e-mail: deposit@ccdc.cam.ac.uk or http://www.ccdc.cam.ac.uk).

Acknowledgements

The financial assistance by the University Grants Commission, New Delhi, India is gratefully acknowledged. P.S. is grateful to the Council of Scientific and Industrial Research, New Delhi, India for the award of JRF.

References

[1] N.W. Alcock, Adv. Inorgchem. Radiochem. 15 (1972) 1.

[2] (a) Reviews concerning intermolecular SBIs involving Te: J. Zukerman-Schpector, I. Haiduc, Phosphorus Sulfur Silicon 171 (2001) 73;
(b) I. Haiduc, J. Zukerman-Schpector, Phosphorus Sulfur Silicon 171 (2001) 171;
(c) J. Zukerman-Schpector, I. Haiduc, Cryst. Eng. Commun. 4 (2002) 178;
(d) A.F. Cozzolino, I. Vergas-Baca, S. Mansour, A.H. Mahmoudkhani, J. Am. Chem. Soc. 127 (2005) 3184;
(e) I. Vergas-Baca, T. Chivers, Phosphorus Sulfur Silicon Relat. Elem. 164 (2000) 164.

[3] (a) Reviews concerning intramolecular SBIs involving Te: W.R. McWhinnie, Phosphorus Sulfur Silicon 67 (1992) 107;
(b) N. Sudha, H.B. Singh, Coord. Chem. Rev. 135/136 (1994) 469;
(c) W.R. McWhinnie, I.D. Sadekov, V.I. Minkin, Sulfur Reports 18 (1995) 295;
(d) V.I. Minkin, I.D. Sadekov, B.B. Rivkin, A.V. Zakharov, V.L. Nivorozhkin, O.E. Kompan, Y.T. Struchkov, J. Organomet. Chem. 536–537 (1997) 233;
(e) I.D. Sadekov, V.I. Minkin, A.V. Zakharov, A.G. Sterikov, G.S. Borodkin, S.M. Aldoshin, V.V. Tkachev, G.V. Shilov, F.J. Berry, J. Organomet. Chem. 690 (2005) 103.

[4] (a) S.D. Apte, S.S. Zade, H.B. Singh, R.J. Butcher, Organometallics 22 (2003) 5473;
(b) S.C. Menon, H.B. Singh, R.P. Patel, S.K. Kulshreshtha, J. Chem. Soc., Dalton Trans. (1996) 1203.

[5] (a) M.R. Greaves, T.A. Hamor, B.J. Howlin, T.S. Lobana, S.A. Mbogo, W.R. McWhinnie, D.C. Povey, J. Organomet. Chem. 420 (1991) 327;
(b) S.A. Mbogo, W.R. McWhinnie, T.S. Lobana, J. Organomet. Chem. 384 (1990) 115.

[6] (a) B.L. Khandewal, A.K. Singh, V. Srivastava, Polyhedron 9 (1990) 2041;
(b) F.W.B. Einstein, C.H.W. Jones, T. Jones, R.D. Sharma, Inog. Chem. 22 (1983) 3924.

[7] (a) A.K.S. Chauhan, A. Kumar, R.C. Srivastava, R.J. Butcher, J. Organomet. Chem. 658 (2002) 169;
(b) A.K.S. Chauhan, A. Kumar, R.C. Srivastava, J. Beckmann, A. Duthie, R.J. Butcher, J. Organomet. Chem. 689 (2004) 345;
(c) A.K.S. Chauhan, Anamika, A. Kumar, R.C. Srivastava, R.J. Butcher, J. Organomet. Chem. 690 (2005) 313.

[8] A.K.S. Chauhan, Anamika, A. Kumar, R.C. Srivastava, R.J. Butcher, J. Beckmann, A. Duthie, J. Organomet. Chem. 690 (2005) 1350.

[9] P. Kerkoc, S. Lochran, R.T. Bailey, F.R. Cruickshank, D. Pugh, J.N. Sherwood, A.J. Blake, J. Appl. Phys. 81 (1997) 624–630, and references therein.
[10] T. Allman, R.G. Goel, Can. J. Chem. 60 (1982) 717.
[11] (a) G.D. markham, C.L. Bock, M. Trachtman, C.W. Bock, J. Mol. Struct. (Theochem.) 459 (1999) 187;
(b) O. Niyomura, S. Kato, S. Inagaki, J. Am. Chem. Soc. 122 (2000) 2132.
[12] (a) A.K. Singh, M. Kadarkaraisamy, G.S. Murthy, J. Srinivas, B. Varghese, R.J. Butcher, J. Organomet. Chem. 605 (2000) 39;
(b) A.K. Singh, J. Sooriyakumar, M. Kadarkaraisamy, J.E. Drake, M.B. Hursthouse, M.E. Light, R.J. Butcher, J. Chem. Res. (S) (2001) 339;
(c) A.K. Singh, J. Sooriyakumar, R.J. Butcher, Inorg. Chim. Acta 312 (2001) 163;
(d) R. Kumar, A.K. Singh, R.J. Butcher, P. Sharma, Eur. J. Inorg. Chem. (2004) 1107.
[13] (a) M.W. Hosseini, Acc. Chem. Res. 38 (2005) 313;
(b) M.W. Hosseini, Cryst. Eng. Commun. 6 (2004) 318;
(c) H. Henry, M.W. Hosseini, New J. Chem. 28 (2004) 897;
(d) S. Mann, Nature 365 (1993) 499.
[14] G.R. Desiraju, Angew. Chem., Int. Ed. Engl. 34 (1995) 2311.
[15] N. Al-Salim, T.A. Hamor, W.R. McWhinnie, J. Chem. Soc., Chem. Commun. (1986) 453.
[16] G. Aullon, D. Bellamy, L. Brammer, E.A. Bruton, A.G. Orpen, Chem. Commun. (1998) 653.
[17] P.K. Thallapally, A. Nangia, Cryst. Eng. Commun. 3 (2001) 114.
[18] V. Balamurugan, M.S. Hundai, R. Mukherjee, Chem. Eur. J. 10 (2004) 1683.
[19] V. Balamurugan, R. Mukherjee, Cryst. Eng. Commun. 7 (2005) 337.
[20] V. Balamurugan, W. Jacob, J. Mukherjee, R. Mukherjee, Cryst. Eng. Commun. 6 (2004) 396.
[21] A. Jouaiti, M.W. Hosseini, A.D. Cian, Chem. Commun. (2000) 1863.
[22] M.J. Collins, J.A. Ripmeester, J.F. Sawyer, J. Am. Chem. Soc. 109 (1987) 4113.
[23] SMART, SAINT, SADABS, Siemens Analytical X-ray Instruments, Inc., Madison, WI, USA, 1999.
[24] L.J. Farrugia, J. Appl. Crystallogr. 32 (1999) 837.
[25] DIAMOND V2.1d, Crystal Impact, K. Brandenburg, M. Berndt GbR. Available from: <http://www.crystalimpact.de>.